FULL PAPER

PPS www.rsc.org/pps

The deactivation pathways of the excited-states of the mycosporine-like amino acids shinorine and porphyra-334 in aqueous solution

Federico R. Conde,[a] M. Sandra Churio*[a,c] and Carlos M. Previtali[b,c]

[a] *Departamento de Química, Facultad de Ciencias Exactas y Naturales, Universidad Nacional de Mar del Plata, Funes 3350, (7600) Mar del Plata, Argentina. E-mail: schurio@mdp.edu.ar*

[b] *Departamento de Química, Universidad Nacional de Río Cuarto, (5800) Río Cuarto, Argentina*

[c] *Consejo Nacional de Investigaciones Científicas y Técnicas (CONICET), Argentina*

Received 19th April 2004, Accepted 28th July 2004
First published as an Advance Article on the web 6th September 2004

In vitro studies on the structurally related mycosporine-like amino acids (MAAs) porphyra-334 and shinorine in aqueous solutions were carried out aiming at their full photochemical and photophysical characterization and expanding the evidence on the assigned UV-photoprotective role of the molecules *in vivo*. The experiments on shinorine confirmed a high photostability and a poor fluorescence quantum yield, in concordance with previous results on porphyra-334. The estimation of triplet production quantum yields for both MAAs was achieved by laser-flash photolysis measurements. In particular, photosensitization experiments on porphyra-334 support the participation of the triplet state in the photodecomposition mechanism yielding a more precise value of Φ_T. As well, photoacoustic calorimetry experiments allowed the first direct quantification of the nonradiative relaxation pathways of the excited MAAs in solution, corroborating that the vast majority (*ca.* 97%) of the absorbed energy is promptly delivered to the surroundings as heat, consistently with the low photodecomposition and emission yields observed.

Introduction

The synthesis and accumulation of UV-absorbing compounds in living organisms has been the subject of intensive research during the last years.[1–4] In particular, mycosporine-like amino acids (MAAs) are generally referred as photoprotective molecules on the basis of their high UV absorption efficiency and the experimentally observed correlation between concentration in a variety of organisms and their exposure to UV radiation.[5–10]

In order to assess the UV-protective effectiveness of these natural 'sunscreens', the photochemical and photophysical properties of these molecules must be characterized.

Three studies on this subject have been previously published, two by Shick *et al.* and the other one by ourselves, reporting respectively the excited-state properties of the imino-MAAs shinorine and porphyra-334 *in vitro*.[11–13] Despite the intense absorption of these MAAs in the UV range, the low quantum yields for fluorescence emission and photolysis together with the absence of photoinduced production of reactive intermediates are consistent with a dominant thermal dissipation of the absorbed energy.[12,13] However, to our knowledge, the direct determination of the nonradiative deactivation yields in MAAs has not been carried out yet.

Photothermal methods are the techniques of choice in order to achieve straight quantification of the thermal contribution to relaxation of excited molecules in solution.[14,15] In particular, photoacoustic calorimetry (PAC) permits the monitoring of delivery of heat from deactivation processes occurring in liquids between some nanoseconds and a few microseconds after photon absorption. The detection is based on the use of piezoelectric elements which follow the pressure changes upon the release of heat pulses in the condensed medium.[14–16]

In this report we focus on the results of the experimental study of the photophysical and photochemical behavior of the structurally-related MAAs shinorine and porphyra-334 (Scheme 1) associated with the various – radiative and nonradiative – deactivation modes of the excited species in aqueous solution. The data are compared with those already obtained in our previous work on porphyra-334.[12] Also new determinations on this MAA were performed in order to reevaluate the fluorescence and triplet quantum yields and to quantify its nonradiative deactivation rate.

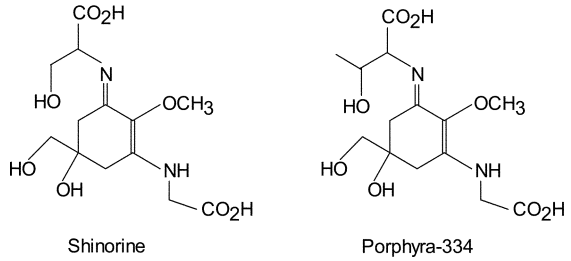

Scheme 1

Finally, the information derived from this set of *in vitro* studies may contribute to understand the dynamics of MAA production and environmental control of MAA synthesis. As an example of this strategy, even pondering the inherent difficulties of *in vitro* to *in vivo* extrapolations, the recently examined *in vitro* photoisomerization of the MAAs usujirene and palythene has enabled the outlining of its role on the transformation of MAAs in organisms.[17]

Experimental

Materials

Shinorine and porphyra-334 were isolated from the red macroalga *Porphyra leucosticta* as described in a previous report.[12] In this case, the final purification step by HPLC was repeated twice, increasing purity up to >99%. Preliminary assignation of chemical structures of the MAAs obtained by HPLC fractionation was achieved by alkaline hydrolysis, identification and subsequent quantification of the hydrolyzed amino acids

DOI: 10.1039/b405782a

by derivatization with *o*-phthalaldehyde.[18] Molecular identities were confirmed by proton magnetic resonance (^{1}H-NMR) and by HPLC-cochromatography with standard samples. The spectrum acquired for shinorine agrees with that one reported by Tsujino,[19] whereas for porphyra-334 it was coincident with the shifts reported by Takano.[20,12]

Sample solutions were stored in the dark at −14 °C. Concentrations of porphyra-334 and shinorine were estimated from the UV absorbances on the basis of the literature molar absorption coefficients at 334 nm: ε (shinorine) = 4.47×10^4 M^{-1} cm^{-1} and ε (porphyra-334) = 4.23×10^4 M^{-1} cm^{-1}.[19,20]

1-Naphtalene-methanol (NMe) from Aldrich, indigo carmine (IC) and quinine bisulfate, from Sigma-Aldrich, were used without further purification. Sodium chloride was analytical grade from Merck. Acetone and acetonitrile, PA reactants from Sintorgan, were used as received. Phenylglyoxylic acid (PGA) from Sigma was recrystallized from PA carbon tetrachloride (Dorwill) and stored in a desiccator in the dark. Water was Millipore Milli-Q grade.

Methods

Unless otherwise indicated, UV-visible absorption spectra were recorded on a Shimadzu UV-2001PC scanning spectrophotometer in quartz cuvettes with 1cm path length. Absorbances were registered with a precision of ± 0.005 units. HPLC analysis of MAAs were carried out as already described.[12]

Photostability studies on aqueous solutions of *ca.* 1.5×10^{-5} M shinorine at room temperature were carried out in a home-made merry-go-round photoreactor with two low-pressure 4 W UV-B lamps (TUV lamp F4T5BL / 4W UV-B Philips). For the determination of photodegradation quantum yields, the MAA porphyra-334 in water was used as the actinometer under the same experimental conditions of shinorine studies. In the cases of the experiments under O_2 or N_2 atmospheres, both sample and actinometer solutions were previously bubbled with the corresponding gas for 20 min and kept in perfectly closed quartz cells during irradiation.

For the photosensitization experiments on porphyra-334, aqueous solutions containing 1.0×10^{-5} to 2.0×10^{-4} M porphyra-334 and *ca.* 2.3×10^{-3} M NMe, were irradiated in the merry-go-round photoreactor now equipped with 4 W germicidal lamps (G4T5 / 4 W Osram). The actinometry was achieved by monitoring the absorbance bleaching of 0.025 M PGA in acetonitrile–water 3 : 1 at 380 nm. The reaction quantum yield was taken as 0.63 from the linear interpolation of the values reported by Defoin *et al.*[21] Porphyra-334/sensitizer and actinometer solutions were previously bubbled with N_2.

Steady-state fluorescence spectra were measured on a Spex Fluoromax spectrofluorimeter. Corrected excitation and emission spectra were recorded with 2 mm slits in order to optimize the signal to noise ratio, also the signal obtained for the solvent was subtracted. For the determination of quantum yields and in order to avoid signal saturation of the quinine bisulfate used as the fluorescence reference, the fluorescence spectra were obtained with 1 mm slits. Concentrations of the MAAs were 6.0×10^{-6} M for porphyra-334 and 6.1×10^{-6} M for shinorine in aqueous solution, respectively. In the case of porphyra-334, the quantum yield was referred to that of the quinine bisulfate in 0.5 M sulfuric acid ($\Phi_F = 0.546$)[22] by comparison of the respective integrated fluorescence spectra, whereas for shinorine the area comparison was made with the fluorescence spectrum of porphyra-334.

Fluorescence lifetimes were measured on an Edinburgh Instruments OB900 time-correlated single photon counting fluorimeter. The analysis of the decays was performed with the software provided by Edinburgh Instruments.

The details concerning the laser flash photolysis (LFP) system used for the characterization of the triplet states are described elsewhere.[12]

Experimental set-up for the PAC measurements is the same as that one used by Brusa *et al.*[23] The laser beam went through a 0.5 mm-width rectangular slit, therefore the acoustic transit time, *i.e.* the heat integration time for the prompt signals, amounted to less than 1 μs (0.34 μs for neat water).[14] IC was employed as the calorimetric reference.[24] As a consequence of the isolation procedure, MAAs aqueous samples carry residual quantities of dissolved ions which were present in the HPLC mobile phase, both sample and reference solutions were prepared in 0.1 M NaCl in order to obtain equivalent thermoelastic parameters. The absorbances of sample and reference solutions were matched at a value *ca.* 0.25 at the laser wavelength and measured in a Hewlett Packard 54504 spectrophotometer with a maximal error of 4%. The temperature was registered directly inside the solutions to ±0.1 K with a Digi-Sense thermistor coupled to a YSI-model 702A temperature probe, and it was varied between 279 and 298 K. In all the cases, the amplitude of the photoacoustic signals varied linearly with the absorbed laser energy, the latter amounting mostly to 0.1 mJ.

Results

Photostability

The MAA concentration decay of aqueous solutions of shinorine *ca.* 1.54×10^{-5} M under UV-B irradiation was followed by UV absorption spectroscopy and HPLC analysis of the aliquots taken before and after irradiation. Quantitative analysis by HPLC indicated the absence of photoproducts absorbing in the range of shinorine absorption spectra.

Besides, the thermal stability of the solutions was also checked. Neutral to slightly acid (pH ≈ 6) aqueous solutions of shinorine probed to be very stable in the dark and below 45 °C.

Fig. 1 shows the changes of the absorbance spectra of aqueous shinorine at different irradiation times. A plot of the maximal absorbance of the solution (at 334 nm) *vs.* irradiation time (not shown) led to the estimation of the initial photolysis rate, v_i^S, as the initial slope of the curve. Analogously, the initial photolysis rate, v_i^P, of an aqueous solution of porphyra-334 of the same absorbance was determined under the same experimental conditions. Thus, porphyra-334 served as a proper actinometric reference since its absorption spectra completely overlaps that one of shinorine.[12]

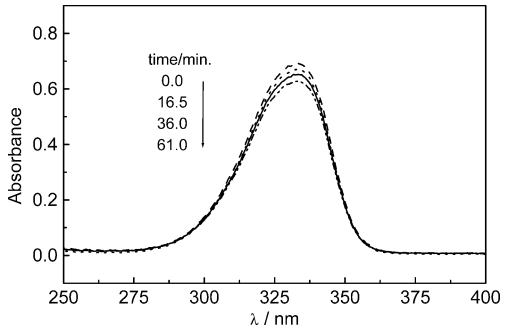

Fig. 1 Stationary UV-photolysis of shinorine in aqueous solution under air atmosphere. Each curve corresponds to the absorption spectrum of the solution after a different irradiation time as indicated on the left.

The photodecomposition quantum yields of shinorine, Φ_R^S, were calculated according to eqn. (1):

$$\Phi_R^S = \frac{v_i^S}{v_i^P}\Phi_R^P \qquad (1)$$

where Φ_R^P denotes the photodecomposition quantum yield of porphyra-334 in aqueous solutions under equivalent experimental conditions.[12] The results are summarized in Table 1.

Table 1 Photodecomposition quantum yields of shinorine Φ_R^S, and porphyra-334 Φ_R^P, in aqueous solution under different experimental conditions

Φ_R^S	$\Phi_R^{P\,a}$	Experimental conditions
$(3.1 \pm 0.7) \times 10^{-4}$	$(1.9 \pm 0.3) \times 10^{-4}$	Under N_2 atmosphere
$(3.4 \pm 0.5) \times 10^{-4}$	$(2.4 \pm 0.3) \times 10^{-4}$	Under air atmosphere
$(4.9 \pm 0.8) \times 10^{-4}$	$(3.4 \pm 0.4) \times 10^{-4}$	Under O_2 atmosphere

[a] Determined in a previous work.[12]

Steady-state spectra and fluorescence quantum yield

The steady-state absorption, emission and excitation spectra for shinorine 6.1×10^{-6} M are shown in Fig. 2. The spectra are corrected by blank subtraction, since due to the very low emission intensity of the samples, Rayleigh and Raman scattering made an important contribution to the emission. The weak and structureless emission band with a maximum at 386 nm, was obtained by excitation at 334 nm. The excitation spectrum was monitored at 460 nm. Considering its low intensity, this spectrum shows a reasonable coincidence with the absorption band, mainly on the long wavelength side.

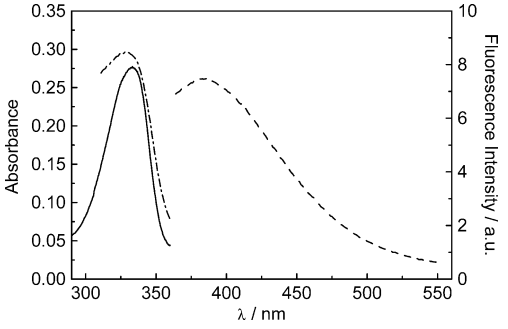

Fig. 2 Absorption (——), emission (---) and excitation (-·-) spectra of aqueous 6.0×10^{-6} M shinorine. Emission spectrum was obtained by excitation at 334 nm. For the excitation spectrum, the emission was observed at 460 nm. The vertical axis on the left corresponds to the absorption spectrum, and that on the right is associated with the emission and the excitation spectra.

The measurement of the fluorescence quantum yield for shinorine was based on the recalibrated value for porphyra-334 as described in the experimental section. In this case, the emission was obtained by excitation at 350 nm. The results are displayed in Table 2.

Excited-singlet state lifetime

The time-correlated single photon counting method was employed for the determination of the fluorescence decay at 420 nm of an air-saturated aqueous solution of shinorine *ca.* 5×10^{-6} M. Excitation of the sample at room temperature was carried out with 330 nm UV-radiation.

One of the resulting temporal evolution of the emitted photon counts is represented in Fig. 3. The decay was fitted with a bi-exponential function. The major component, with a lifetime of 0.35 ± 0.10 ns was ascribed to the emission of shinorine. The second decay, with a lifetime of 6.6 ns and a relative weight of *ca.* 1% in the decay function, was assigned to impurities in the sample.

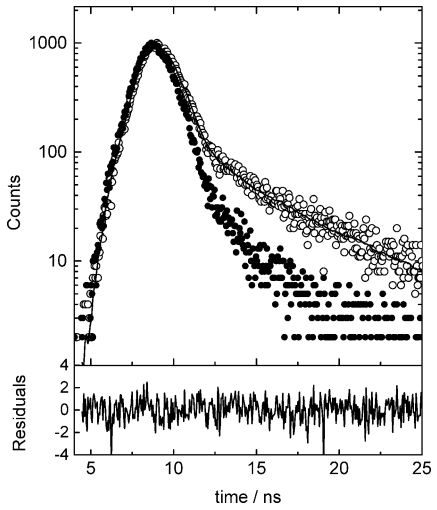

Fig. 3 Time-resolved fluorescence of shinorine under air atmosphere measured by single-photon counting. Shinorine concentration was 5×10^{-6} M in water. The excitation was carried out at 330 nm and the emission was registered at 420 nm. Full circles describe the signal from the excitation source, open circles represent the signal from the sample. Residuals correspond to the fitting of the sample signal to a bi-exponential decay function (solid line).

Triplet state characterization

The triplet state of porphyra-334 in aqueous solution has been previously studied by sensitized LFP with various donors at 266 nm, since direct excitation of 6×10^{-5} M solutions at 355 nm yielded no absorption transient.[12]

In this work, the characterization of the excited-triplet state of shinorine was also carried out by LFP experiments on aqueous solutions of the molecule. Although the direct excitation of 5.8×10^{-5} M shinorine at 355 nm produced no transient signal in the microseconds time range, within the detection limit of the experimental set-up, a transient absorption between 350 and 550 nm could be observed by sensitization with acetone. In this case, the experiment was carried out on a 4.7×10^{-5} M shinorine solution in the presence of 3.45×10^{-2} M acetone and 266 nm laser irradiation. Under these conditions, the laser pulses are mostly absorbed by acetone.

From the absorbance decays at various observation wavelengths, the transient spectra at different times after the laser pulse were constructed. Some data are presented in Fig. 4 which exhibits the maximal absorption building up around 420 nm and *ca.* 5 μs (not shown) after the laser pulse. For comparison purposes, the spectrum is displayed together with the triplet–triplet absorption band measured for aqueous porphyra-334.[12] Although both spectra were taken under different intensity conditions of the analyzing beam, explaining the distinct scales in the vertical axis, it is clear that the absorption profiles share similar characteristics as for instance the maximal absorption wavelength.

In addition, a blank experiment was performed by excitation of acetone solutions with the same concentration used in the former experiment. At various time intervals after the laser pulse, the observed transient spectra extend from 280 to 360 nm (not shown) and were assigned to triplet acetone, in agreement with published data.[25] From the present measurements, the recovered

Table 2 Some photophysical parameters for shinorine (S) and porphyra-334 (P) in aqueous solution

	Shinorine	Porphyra-334
Fluorescence quantum yield	$\Phi_F^S = (1.6 \pm 0.2) \times 10^{-4}$	$\Phi_F^P = (2.0 \pm 0.2) \times 10^{-4}$
Fluorescence lifetime/ns	$\tau_F^S \approx 0.35 \pm 0.10$	$\tau_F^P \approx 0.40 \pm 0.05$
Triplet quantum yield	$\Phi_T^S < 0.05$	$\Phi_T^P = 0.030 \pm 0.005$
Triplet lifetime/μs	$\tau_T^S = 11$	$\tau_T^P = 14$

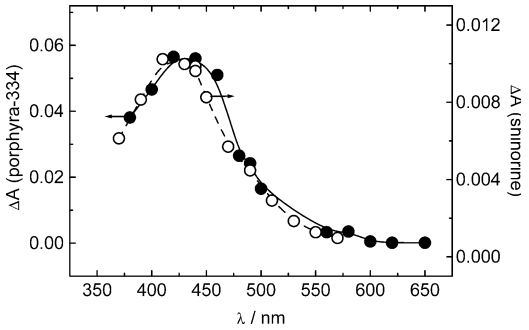

Fig. 4 Triplet–triplet absorption spectra obtained by sensitization of 4.3×10^{-3} M porphyra-334 with 5.7×10^{-5} M benzophenone (●)[12] and of 5.8×10^{-5} M shinorine with 0.0345 M acetone (○) by LFP at 266 nm. Both spectra were taken 2 μs after the laser pulse. Arrows point to the corresponding vertical axis for each spectrum.

lifetime for the excited acetone was *ca.* 4 μs. Besides, from the sensitization experiment at a fixed observation wavelength, the growth and decay of the transient signal was obtained as Fig. 5 shows for 440 nm.

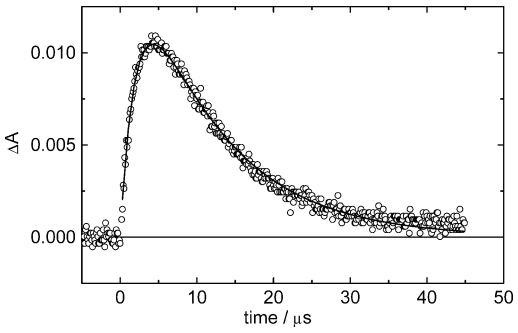

Fig. 5 Time evolution of the absorbance at 440 nm of the triplet state of shinorine obtained by sensitized LFP at 266 nm of 5.8×10^{-5} M shinorine with 0.0345 M acetone in water. Solid line represents the fitting to a bi-exponential decay function.

Regarding porphyra-334, photosensitized degradation experiments were carried out in order to asses the role of triplets in the photodecomposition mechanism. Porphyra-334 concentration was varied between 1.0×10^{-5} to 2.0×10^{-4} M, whereas the photosensitizer NMe was *ca.* 2.3×10^{-3} M in the N_2-purged aqueous solutions. Under these conditions, the indirect photodecomposition quantum yields were determined at each porphyra-334 concentration as previously reported.[12] For this set of experiments, the irradiation emitted by the photolysis lamps concentrates at 253.7 nm were only NMe absorbs, at least within the range of concentrations employed for porphyra-334. The results, compiled in Table 3, were obtained by using PGA as an actinometer.

Photoacoustic calorimetry and nonradiative deactivation pathways

PAC studies allowed for the direct quantification of the nonradiative deactivation pathways of the excited MAAs.

Fig. 6 compares one typical pair of PAC signals obtained for shinorine and for IC, the calorimetric reference, in 0.1 M NaCl at 283.2 K. At first sight, both signals overlap completely and one would conclude that shinorine behaves as IC, *i.e.* it releases promptly all the absorbed energy as heat. Equivalent signal profiles were also observed for porphyra-334 and IC in 0.1 M NaCl at the same temperature (not shown for simplicity).

Table 3 Indirect photodecomposition quantum yields of porphyra-334, Φ_{iR}^{P} at ≈254 nm[a]

[P] / M × 10^{-5}	2.04	2.05	6.80	11.9	12.0	15.0	17.7
Φ_{iR}^{P} / 10^{-4}	7.34	7.56	15.5	21.5	24.1	20.8	28.2

[a] Measured on N_2-purged aqueous solutions in the presence of *ca.* 2.3×10^{-3} M NMe.

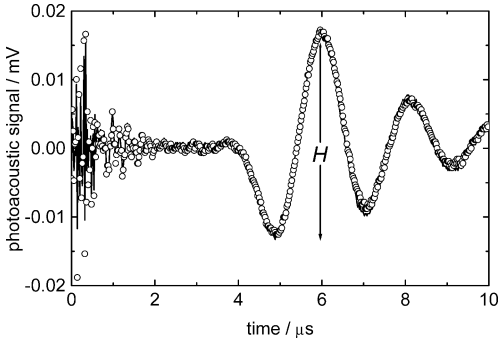

Fig. 6 Photoacoustic signal obtained for 5.5×10^{-6} M shinorine (○) and IC (—) in 0.1 M aqueous NaCl at 283.2 K and 0.083 mJ laser pulse energy. *H* denotes the signal amplitude measured from the maximum to the minimum of the first waveform.

Actually, it has to be considered that two contributions produce a PAC signal: the thermal expansion/contraction of the medium upon the heat delivered through radiationless relaxation, and the concomitant structural volume changes induced in the photoactive species and/or the surrounding solvent. Separation of both contributions may be achieved by temperature-dependent PAC measurements.[14–16,26] The method is based on the determination at different temperatures of the ratio of energy-normalized signal amplitudes H_n for the MAA and for the calorimetric reference, *i.e.* H_n^M/H_n^{ref}. The values of H_n were measured as the slope of the linear plots of *H*, the peak-to-peak distance in the earliest wave of the signal as indicated in Fig. 6, as a function of the laser fluence.

It has been demonstrated that for photoreactions producing permanent products or transient species characterized by lifetimes longer than *ca.* 10 μs, this ratio can be described in terms of the thermoelastic properties of the media according to the following expression:[14–16,26]

$$\frac{H_n^M}{H_n^{ref}} = \alpha + \frac{\Delta V_e}{E_\lambda}\left(\frac{C_p \rho}{\beta}\right) \quad (2)$$

where α is the fraction of the absorbed energy delivered as heat, E_λ is the energy of one mole of photons (one Einstein) of the laser wavelength λ, Δv_e accounts for the structural volume change per absorbed Einstein, C_p denotes the specific heat capacity, ρ is the density and β stands for the thermal expansion coefficient of the solution.

Table 4 shows the results of energy-normalized amplitudes obtained for shinorine and porphyra-334 relative to the calorimetric reference at various temperatures. The data in the second column show that, within the error of the measurements, the ratio H_n^M/H_n^{IC} keeps around unity at each temperature. *A priori*, this may indicate that the MAAs release rapidly all the absorbed energy to the medium as the calorimetric reference does. However, a plot of the ratio of energy-normalized signals

Table 4 Ratios of energy-normalized signals for the MAAs and for IC, the calorimetric reference, and the corresponding value of (C_p ρ/β), the set of thermoelastic parameters for 0.1 M NaCl solutions, at different temperatures

MAA	H_n^M/H_n^{IC}	*T*/K	(C_p ρ/β) / kJ mL^{-1}[a]
Shinorine	0.90 ± 0.10	298.1	14.81
	1.00 ± 0.05	283.1	31.66
	1.11 ± 0.15	279.1	42.18
Porphyra-334	1.12 ± 0.15	298.1	14.81
	1.00 ± 0.05	283.0	31.50

[a] Extracted from Borsarelli *et al.*[38,39]

for shinorine *vs.* the set of the corresponding thermoelastics parameters in the fourth column of Table 4 (Fig. 7) shows a slight positive linear trend. The linear regression of the data, weighed by the experimental error of each ratio H_n^M/H_n^{IC}, renders a slope of $(6.8 \pm 5.7) \times 10^{-3}$ mL kJ^{-1} and an intercept of 0.79 ± 0.17. According to eqn. (2), the first figure corresponds to $\Delta v_e/E_\lambda$ and the intercept provides directly the value of a. Considering that E_λ = 336.9 kJ Einstein^{-1} for $\lambda = 355$ nm, Δv_e affords 2.3 ± 1.9 mL Einstein^{-1}.

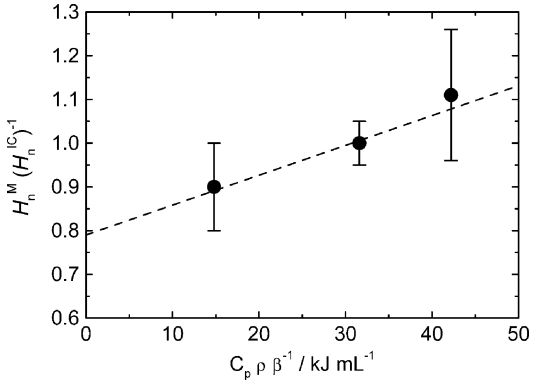

Fig. 7 Ratio of energy-normalized photoacoustic signal amplitudes for shinorine and the calorimetric reference, IC, as a function of the set of thermoelastic parameters (C_p ρ/β) for aqueous 0.1 M NaCl solutions. The dashed line indicates the linear regression of the data weighed by the individual experimental error of the ratio at each temperature (slope = 0.0068 ± 0.0015; intercept = 0.7900 ± 0.0447, $r = 0.9775$).

Discussion

The comparison of the results for the photodecomposition quantum yields in Table 1 reveals that the photodegradation of shinorine in aqueous solution is slightly higher than that measured for porphyra-334 under the same conditions, although both sets of values share the small order of magnitude ($\Phi_R \approx 10^{-4}$) indicating a very high photostability.

The similar magnitudes of Φ_R^S and Φ_R^P are expected on the basis of the strongly related molecular structures (Scheme 1). Besides, the values obtained for Φ_R^S are consistent with the lack of photoreactivity already reported for shinorine by Adams and Shick.[11]

The trend observed in Table 1 for the quantum yields of each MAA under different contents of oxygen may suggest the involvement of reactive molecular oxygen species in the photodecomposition mechanism, but the limited extent of the photodegradation precludes direct exploration of this issue. However, we carried out the generation of $^1O_2$ by photosensitization with Rose Bengal in methanol at 532 nm,[27] and we observed no quenching of the singlet oxygen IR-phosphorescence in the presence of 6.9×10^{-5} M porphyra-334. Still, this negative result does not reject a role of singlet oxygen in the photodegradation of the MAAs. In fact, considering the minimal difference in emission lifetimes that can be detected with the set up of this experiment, we estimated a limit for the quenching constant of $^1O_2$ by the MAA as $k_q < 3.3 \times 10^7$ M^{-1} s^{-1}. This value is similar to the recently determined by Suh *et al.* for the global deactivation of $^1O_2$ by mycosporine glycine in chloroform–methanol 85 : 15, which rendered 5.6×10^7 M^{-1} s^{-1}.[28] In conclusion, the low value of k_q together with the lower lifetime of singlet oxygen in water, make the participation of singlet oxygen in the photodegradation mechanism a very improbable one.[29] Nevertheless, trapping of the cage radicals from a MAA molecule by ground state oxygen can not be discarded.

The improvement achieved in the measurement of the fluorescence spectra by the selection of narrow slits and the double-HPLC step purification of the samples, led to the re-evaluation of Φ_F^P, the fluorescence quantum yield for porphyra-334 in water. The new value is one order of magnitude lower than that one determined in our previous work and compares better with the value obtained for Φ_F^S, the fluorescence quantum yield for shinorine in water (see Table 2).[12] This low yield is in turn in line with the results reported by Shick *et al.* for aqueous shinorine.[13] Thus, the last determination of Φ_F^P seems to give a more reasonable result in terms of the molecular structures of both MAAs. In summary, both quantum yields denote a very weak emission which offers no support to the energy transfer from this fluorescence to chlorophylls that has been suggested on the basis of the overlapping of the emission spectrum of the MAAs and the Soret band of chlorophylls.[30,31] However, MAAs may work as photosynthetic antennas transferring energy to chlorophylls through a Förster-type nonradiative mechanism,[32] since it has not been ruled out the MAAs to be located close to the chlorophylls within the photosynthetic apparatus.[33]

As already found for porphyra-334,[12] the brief excited singlet state lifetime determined for shinorine by single photon counting (see Table 2), is in good agreement with the small magnitude of the fluorescence quantum yield.

The sensitization LFP experiments of shinorine with acetone (Fig. 4) are in line with an energy transfer process from the triplet acetone. According to this hypothesis, the assumed mechanism is described by eqn. (3) to (6):

$$A \xrightarrow{h\nu} {}^3A^* \quad (3)$$

$${}^3A^* \xrightarrow{k_D^A} A \quad (4)$$

$${}^3A^* + S \xrightarrow{k_q^{A,S}} {}^3S^* + A \quad (5)$$

$${}^3S^* \xrightarrow{k_D^S} S \quad (6)$$

where A and ^{3}A* denote ground state and triplet state acetone respectively, and correspondingly S and ^{3}S* stand for ground and triplet state shinorine. Thus, the absorption of one photon of the laser pulse, symbolized in eqn. (3) by *hν*, promotes with maximal efficiency one acetone molecule to the excited triplet state (Φ_T = 1).[34] Acetone in turn, deactivates back to the ground state either with a first order constant k_D^A [eqn. (4)] or by quenching by shinorine with a second order constant $k_q^{A,S}$, in this case generating excited triplet state shinorine [eqn. (5)]. Finally, the excited shinorine decays with an overall first order constant k_D^S [eqn. (6)].

On contrasting this model with the experimental results, the transient signals of the blank experiment with acetone are assigned to ^{3}A*, in agreement with literature data.[25] Consequently, these signals, rising beyond 360 nm towards shorter wavelengths, reinforce that the transitory with maximal absorption at 420 nm in Fig. 4 is originated by ^{3}S* and correspond to a triplet–triplet absorption spectra of shinorine. Furthermore, the trace registered at 440 nm (Fig. 5) clearly shows the growth and decay of the transient signal which can be described in terms of two-step consecutive kinetics involving ^{3}S* as an intermediate, *i.e.* the scheme depicted together by eqn. (4) to (6). Thus, in the first step ^{3}S* is formed by energy transfer from ^{3}A*, which may alternatively decay with an apparent kinetic constant $k_1 = k_D^A + k_q^{A,S}$ [S], entailing the growth of the signal. The coupled second step involves the decay of ^{3}S* to the ground state (the decrease of the signal) and is described by the first order constant $k_2 = k_D^S$. Hence, as stated above, the signal can be analytically expressed in terms of the concentration of ^{3}S* as a function of time, according to the consecutive kinetics as shown by eqn. (7):

$$[{}^3S^*] = \frac{[{}^3A^*]k_1}{k_2 - k_1} [\exp(-k_1 t) - \exp(-k_2 t)] \quad (7)$$

The fit of the trace in Fig. 5 to this expression affords $k_1 = 4.8 \times 10^5$ s^{-1} and $k_2 = 9.1 \times 10^4$ s^{-1}. From k_1, and considering the experimentally determined lifetime of $^3A^*$, $\tau_T^A = (k_D^A)^{-1} = 4$ μs, and the concentration of shinorine (5.8×10^{-5} M), the value of

$k_q^{A,S}$ results *ca.* 4×10^9 $M^{-1}s^{-1}$ which corresponds to a diffusion-controlled process for neutral species in water.[34] From k_2, the lifetime of triplet shinorine was calculated as $\tau_T^S = 11$ μs.

This kinetic information enables to evaluate that almost 50% of the excited acetone promotes shinorine to the triplet state, confirming the high efficiency of the energy transfer between acetone and shinorine. Additionally, taking into account the estimated detection limit of the LFP device ($\Phi_T \varepsilon_T > 500$ M^{-1} cm^{-1}), the absence of triplet absorption signal from direct excitation of shinorine indicates that $\Phi_T^S < 0.05$. This evaluation rests on the assumption of a maximum molar absorption coefficient ε_T^S for triplet shinorine of the same magnitude as the value for triplet porphyra-334 at 440 nm, $\varepsilon_T^P \approx 10^4$ M^{-1} cm^{-1}.[12] The result for Φ_T^S also agrees with the previously estimated quantum yield Φ_T^P for porphyra-334.[12] However, a more precise value for Φ_T^P could be retrieved from the results obtained in the photosensitized decomposition of porphyra-334 (Table 3) as described in the following paragraphs.

Eqn. (8) to (14) show the mechanism proposed for the indirect photodecomposition of porphyra-334 sensitized by NMe in O_2-free solutions:

$$\mathrm{NMe} \xrightarrow{h\nu} {}^1\mathrm{NMe}^* \quad (8)$$

$${}^1\mathrm{NMe}^* \xrightarrow{{}^1k_D^{NMe}} \mathrm{NMe} \quad (9)$$

$${}^1\mathrm{NMe}^* \xrightarrow{k_{ISC}^{NMe}} {}^3\mathrm{NMe}^* \quad (10)$$

$${}^3\mathrm{NMe}^* \xrightarrow{{}^3k_D^{NMe}} \mathrm{NMe} \quad (11)$$

$${}^3\mathrm{NMe}^* + \mathrm{P} \xrightarrow{k_q^{NMe,P}} N\mathrm{Me} + {}^3\mathrm{P}^* \quad (12)$$

$${}^3\mathrm{P}^* \xrightarrow{k_R^P} \mathrm{X} \quad (13)$$

$${}^3\mathrm{P}^* \xrightarrow{{}^3k_D^P} \mathrm{P} \quad (14)$$

The first event of this reaction scheme is the absorption of photon energy by the sensitizer [eqn. (8)] producing the excited singlet state of NMe, denoted as ^{1}NMe*. In the following steps, ^{1}NMe* deactivates to ground state [eqn. (9)] or yields the triplet state ^{3}NMe*, *via* intersystem crossing [eqn. (10)]. ^{3}NMe* may also decay through an unimolecular process [eqn. (11)] and as a result of quenching by porphyra-334, P, [eqn. (12)]. The last process, which sensitizes the promotion of this molecule to the triplet state ^{3}P*, has been directly observed by LFP leading to the value for the rate constant $k_q^{NMe,P} = (4.8 \pm 0.4) \times 10^8$ M^{-1} cm^{-1}.[12] Part of this excited porphyra-334 reacts yielding the photodecomposition product or products symbolized in eqn. (13) with an X, and the rest decays to ground state [eqn. (14)]. The mechanism does not include the quenching of ^{1}NMe* by P, consistently with the short lifetime of ^{1}NMe* and the low concentration of P in the experiments.[12]

The kinetic analysis of the last set of reactions leads to the expression in eqn. (15), relating a series of kinetics constants with the indirect photodecomposition quantum yield, Φ_{iR}^P:

$$\frac{1}{\Phi_{iR}^P} = \frac{1}{\Phi_T^{NMe}} \left(\frac{k_R^P + {}^3k_D^P}{k_R^P} \right) \left(1 + \frac{{}^3k_D^{NMe}}{k_q^{NMe,\ \&\ P}} \frac{1}{[P]} \right) \quad (15)$$

where Φ_T^{NMe} states for the NMe triplet quantum yield, and ${}^3k_D^{NMe}$, $k_q^{NMe,P}$, k_R^P and ${}^3k_D^P$ correspond, respectively, to the rate constants of the reactions described by eqn. (11) to (14).

The results in Table 3 verify this relationship as shown by the linear dependence obtained in the plot of $1/\Phi_{iR}^P$ *vs.* 1/[P] in Fig. 8, thus supporting the implication of the excited triplet state in the photodecomposition of porphyra-334, according to the proposed mechanism [eqn. (8)–(14)].

From the linear correlation of the experimental values in Fig. 8, the intercept yields $k_R^P/(k_R^P + {}^3k_D^P) = (6.2 \pm 0.6) \times 10^{-3}$, assuming for Φ_T^{NMe} the amount from the literature of the triplet quantum yield of 1-methylnaphthalene, $\Phi_T^{MeN} = 0.58$.[34] Also, the value of $k_q^{NMe,P}$ was derived from the ratio

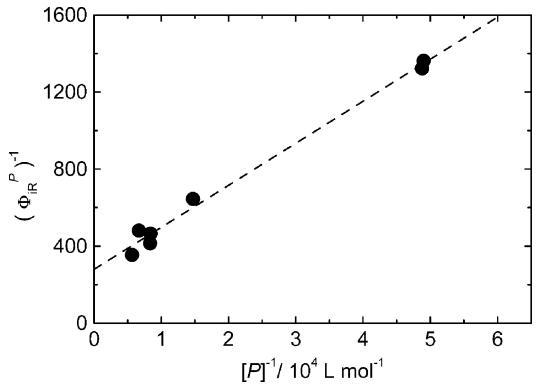

Fig. 8 Plot of the inverse of the indirect photodecomposition quantum yield of porphyra-334 in aqueous solution *vs.* the inverse of porphyra-334 concentration. Data extracted from Table 3. Dashed line shows the linear fitting of the experimental data (slope = 0.0218 ± 0.0004; intercept = 279.5398 ± 25.4431; r = 0.9955).

of the slope and the intercept from the linear regression of Fig. 8, and taking into account the lifetime of triplet NMe from our previous work, *i.e.* $\tau_T^{NMe} = ({}^3k_D^{NMe})^{-1} = 2.2 \times 10^{-5}$ s.[12] In this way, we estimate $k_q^{NMe,P} = 5.8 \times 10^8$ M^{-1} s^{-1} which is very close to the value determined from direct measurements (see above).[12]

On the other hand, a basic mechanism is proposed for the direct photodegradation of porphyra-334 in the absence of oxygen. In this mechanism, the excited singlet state porphyra-334, ^{1}P*, formed by photon absorption in the first step [eqn. (16)] may deactivate back to ground state by nonradiative and radiative (fluorescence) pathways, globally represented by eqn. (17), with an overall rate constant k_D^P.

$$\mathrm{P} \xrightarrow{h\nu} {}^1\mathrm{P}^* \quad (16)$$

$${}^1\mathrm{P}^* \xrightarrow{k_D^P} \mathrm{P} \quad (17)$$

A fraction of ^{1}P* molecules may also undergo intersystem crossing to the triplet state with a rate constant k_{ISC}^P, as eqn. (18) shows.

$${}^1\mathrm{P}^* \xrightarrow{k_{ISC}^P} {}^3\mathrm{P}^* \quad (18)$$

Again, the fate of these triplets is that one proposed for the indirect photodecomposition mechanism by eqn. (13) and (14).

It is worth noting that the mechanism for the direct photodecomposition assumes that ^{1}P* is not involved in the photochemistry, *i.e.* no product is obtained from this excited state. This hypothesis is based in the very short lifetime of the excited singlet state estimated from the fluorescence measurements (see Table 2). However, considering the mentioned singlet lifetime and the measured photoreaction quantum yields (see Table 1), one can estimate that a potential decomposition pathway from the excited-singlet state might compete with the rapid nonradiative decays to ground state or to the triplet state with a rate constant amounting to as much as *ca.* 5×10^5 s^{-1}. This value is much larger than the rate constant for the photoreaction from triplet state, determined from the proposed mechanism to be 4.4×10^2 s^{-1} on the basis of the value derived for $k_R^P/(k_R^P + {}^3k_D^P)$ and the τ_T^P from Table 2. Nevertheless, if this higher reaction rate constant from the singlet were operative, one should expect the direct photodecomposition to be more efficient in comparison to that observed from triplet–triplet energy transfer experiments (compare data in Tables 1 and 3).

Eqn. (19), derived from the mechanism introduced above, describes the direct photodecomposition quantum yield, Φ_{dR}^P, as a function of kinetics constants and the triplet quantum yield for porphyra-334:

$$\Phi_{dR}^P = \Phi_T^P \left(\frac{k_R^P}{k_R^P + {}^3k_D^P} \right) \quad (19)$$

Thus, using the value of $k_R^P/(k_R^P + {}^3k_D^P)$ previously evaluated from the photosensitized decompositions (Fig. 8), Φ_T^P can be obtained from eqn. (19) as

$$\Phi_T^P = \Phi_{dR}^P \left(\frac{k_R^P + {}^3k_D^P}{k_R^P} \right).$$

In consequence, considering the result for the photodecomposition quantum yield of porphyra-334 in N_2 atmosphere from Table 1, $\Phi_{dR}^P = 1.9 \times 10^{-4}$, Φ_T^P yields 0.030 ± 0.005. This result clearly improves the precision of the value $\Phi_T^P < 0.05$, determined in our previous work, and explains the absence of transient signals within the microsecond range in the LFP experiments with direct excitation of P.[12]

Finally, as stated before, the direct quantification of the nonradiative pathways of excited shinorine and excited porphyra-334 was assessed by PAC. As triplet states of these MAAs live longer than ≈10 μs, they should be considered as energy-storing species in the PAC experiment. Thus, an energy balance for the relevant processes within this time range can be expressed as follows, considering one mole of photons absorbed by the MAA:[14,16]

$$E_\lambda = \Phi_F E_F + aE_\lambda + \Phi_{st} E_{st} \quad (20)$$

The first term on the right side of eqn. (20) corresponds to the energy emitted as fluorescence, where Φ_F and E_F denote the fluorescence quantum yield and the molar energy of the fluorescence state, respectively. The third term represents the stored energy, expressed by the quantum yield of formation Φ_{st} times the molar energy content E_{st} of the storing species. For our particular case, this third term includes the energy stored by the triplet states of the MAAs living much longer than the heat integration time. Photodegradation products are not considered here since they are supposed to originate later from the triplet state (see above) and, on the other hand, they are formed with a negligible yield (see Table 1), thus eqn. (20) can be rewritten as:

$$E_\lambda = \Phi_F E_F + aE_\lambda + \Phi_T E_T \quad (21)$$

where E_T stands for the molar energy of the triplet state.

As a first approximation, we can neglect the fluorescence term on the basis of the small quantum yield for this pathway (see Table 2), thus eqn. (21) transforms in eqn. (22):

$$E_\lambda \approx aE_\lambda + \Phi_T E_T \quad (22)$$

Consequently, an estimation for the value of a is defined by:

$$a \approx 1 - \left(\frac{\Phi_T E_T}{E_\lambda} \right) \quad (23)$$

Hence, eqn. (23) yields $a \approx 0.98$ for porphyra-334, taking $E_T = 250$ kJ mol^{-1} from Conde *et al.*,[12] $\Phi_T = \Phi_T^P = 0.03$ from the LFP measurements (see Table 2) and $E_\lambda = 336.9$ kJ Einstein^{-1} for $\lambda = 355$ nm. This result indicates a very high efficiency for the nonradiative relaxation of the excited MAA in complete agreement, within their experimental errors, with PAC results (see Table 4). Besides, this conclusion is in line with the upper limit found for a in the linear regression of the PAC data for shinorine (Fig. 7), *i.e.* $a = 0.79 + 0.17 = 0.96$, and correspondingly supports the lower limit for $\Delta v_e = 2.3 - 1.9$ mL Einstein^{-1} $= 0.4$ mL Einstein^{-1}. Since the formation of triplets is assumed as the energy-storing process that produces the volume change, it is valid to relate Δv_e with the triplet quantum yield as $\Delta v_T = \Delta v_e/\Phi_T$, where Δv_T represents the volume change upon the production of one mole of triplets. Thus, considering for shinorine the same triplet quantum yield as for porphyra-334 (*i.e.* $\Phi_T^S \approx \Phi_T^P = 0.03$), we estimate $\Delta v_T \approx 13$ mL mol^{-1}. This reaction volume change may be interpreted as originated by changes in the aqueous solvation sphere around the initial and final species (ground state and triplet state, respectively) with different dipole moments and specific solute–solvent interactions. In addition, the magnitude of this result is consistent with the values associated with the formation of triplets from other ground-state molecules previously reported in the literature.[35–37]

In summary, the results obtained for a through PAC measurements are supported also by the LFP experiments and indicate that around 96 to 98% of the absorbed photon energy by the MAAs shinorine or porphyra-334 is promptly delivered as heat to the medium. This released heat accounts for the thermal relaxation from excited singlet state and intersystem crossing to triplet state MAA, apart from the rapid vibrational relaxation within the excited states. According to this analysis, within the time window of the PAC determinations, the remaining energy is stored by the triplet state of MAA. The results are also consistent with the small quantum yields for photoreaction and radiative decay found for porphyra-334 as well as for shinorine (Tables 1 and 2). Besides, the low quantum yields for triplet production (Table 2) reduce the probability of triplets to generate reactive intermediates which might start further chemical reactions, in agreement with the lack of radical detection reported by Shick *et al.*[13] Therefore, the photochemical and photophysical parameters determined here for the two MAAs, together with their high absorption coefficients in the UV range, reinforce the assigned *in vivo* photoprotective role of this family of compounds. According to the observed qualities, the accumulated MAAs seem to work as simple screening agents by absorbing efficiently the UV radiation that penetrates the cells and releasing this absorbed energy mainly as heat to the surroundings, thus avoiding the on setting of indirect or direct photochemistry in the exposed organisms which may render harmful to living tissues.

Abbreviations

A, acetone; IC, indigo carmine; LFP, laser flash photolysis; MAA(s), mycosporine-like amino acid(s); NMe, 1-naphthalenemethanol; P, porphyra-334; PAC, photoacoustic calorimetry; PGA, phenylglyoxylic acid; S, shinorine.

Acknowledgements

The authors are grateful to María Luz Piriz (Centro Nacional Patagónico, Pto. Madryn, Argentina) who identified the alga species, to Miguel A. Ponce for the ^{1}H-NMR analysis at the Instituto Universitario de Bio-Orgánica (Universidad de La Laguna, Tenerife, Spain), and to Ignacio Dell'Erba for collaboration in the preliminary experiments on photostability of MAAs. FRC wishes to thank supporting from CONICET (Beca de Formación y Postgrado) and Fundación Antorchas (Beca 2001 para las Ciencias). Research grants from Fundación Antorchas (A-13622/13 and 14022/36) are also acknowledged.

References

1 M. Ehling-Schulz, W. Bilger and S. Scherer, UV-B-induced synthesis of photoprotective pigments and extracellular polysaccharides in the terrestrial cyanobacterium *Nostoc commune*, *J. Bacteriol.*, 1997, **179**, 1940–1945.
2 R. P. Sinha, M. Klisch, A. Gröniger and D-P. Häder, Ultraviolet-absorbing/screening substances in cyanobacteria, phytoplankton and macroalgae, *J. Photochem. Photobiol. B: Biol.*, 1998, **47**, 83–94.
3 J. M. Shick and W. C. Dunlap, Mycosporine-like amino acids and related gadusols: Biosynthesis, accumulation, and UV-protective functions in aquatic organisms, *Annu. Rev. Physiol.*, 2002, **64**, 223–262.
4 D. Libkind, P. Perez, R. Sommaruga, M. C. Diéguez, M. Ferraro, S. Brizzio, H. Zagarese and M. van Broock, Constitutive and UV-inducible synthesis of photoprotective compounds (carotenoids and mycosporines) by fresh water yeasts, *Photochem. Photobiol. Sci.*, 2004, **3**, 281–286.
5 J. I. Carreto, V. A. Lutz, S. G. De Marco and M. O. Carignan, Fluence and wavelength dependence of mycosporine-like amino acid synthesis in the dinoflagellate *Alexandrium excavatum*, in *Toxic Marine Phytoplankton*, ed. E. Graneli, L. Edler, B. Sundström and D. M. Anderson, Elsevier, New York, 1990, pp. 275–279.

6 D. Karentz, E. S. Mc Euen, M. C. Land and W. C. Dunlap, Survey of mycosporine-like amino acid compounds in Antarctic marine organisms: potential protection from ultraviolet exposure., *Mar. Biol.*, 1991, **108**, 157–166.
7 F. Garcia-Pichel, Ch. E. Wingard and R. W. Castenholz, Evidence regarding the UV-sunscreen role of a mycosporine-like compound in the cyanobacterium *Gloeocapasa sp.*, *Appl. Environ. Microbiol.*, 1993, **59**, 170–176.
8 S. A. Wängberg, A. Persson and B. Karlson, Effects of UV-B radiation on synthesis of mycosporine-like amino acid and growth in *Heterocapsa triquetra* (Dinophyceae), *J. Photochem. Photobiol. B: Biol.*, 1997, **37**, 141–146.
9 T. Banaszak, M. P. Lesser, I. B. Kuffner and M. Ondrusek, Relationship between ultraviolet (UV) radiation and mycosporine-like amino acids (MAAS) in marine organisms, *Bull. Mar. Sci.*, 1998, **63**, 617–628.
10 W. M. Bandaranayake, Mycosporines. Are they nature's sunscreens?, *Nat. Prod. Rep.*, 1998, **15**, 159–172.
11 N. L. Adams and J. M. Shick, Mycosporine-like amino acids provide protection against ultraviolet radiation in eggs of the green sea urchin *Strongylocentrotus droebachiensis*, *Photochem. Photobiol.*, 1996, **64**, 149–158.
12 F. R. Conde, M. S. Churio and C. M. Previtali, The photoprotector mechanism of mycosporine-like amino acids. Excited-state properties and photostability of porphyra-334 in aqueous solution, *J. Photochem. Photobiol. B: Biol.*, 2000, **56**, 139–144.
13 J. M. Shick, W. C. Dunlap and G. R. Buettner, Ultraviolet (UV) protection in marine organisms II. Biosynthesis, accumulation, and sunscreening function of mycosporine-like amino acids, in *Free Radicals in Chemistry, Biology and Medicine*, ed. T. Yoshikawa, S. Toyokuni, Y. Yamamoto and Y. Naito, OICA International, London, 2000, pp. 215–228.
14 S. E. Braslavsky and G. E. Heibel, Time resolved photothermal and photoacoustic methods applied to photoinduced processes in solution, *Chem. Rev.*, 1992, **92**, 1381–1410.
15 T. Gensch and C. Viappiani, Time-resolved phototermal methods: accesing time-resolved thermodynamics of photoinduced processes in chemistry and biology, *Photochem. Photobiol. Sci.*, 2003, **2**, 699–721.
16 T. Gensch, C. Viappiani and S. E. Braslavsky, in *Encyclopedia of Spectroscopy and Spectrometry*, ed. J. C. Lindon, Academic Press, London, 1999, p. 1124.
17 F. R. Conde, M. O. Carignan, M. S. Churio and J. I. Carreto, *In vitro cis–trans* photoisomerization of palythene and usujirene. Implications on the *in vivo* transformation of mycosporine-like amino acids, *Photochem. Photobiol.*, 2003, **77**, 146–150.
18 W. S. Gardner and W. H. Miller III, Reverse-phase liquid chromatographic analysis of amino acids after reaction with o-phthalaldehyde, *Anal. Biochem.*, 1980, **101**, 61–65.
19 I. Tsujino, K. Yabe and I. Sekikawa, Isolation and structure of a new amino acid, shinorine, from the red alga, *Chondrus yendoi* Yamada et Mikami, *Bot. Mar.*, 1980, **23**, 65–68.
20 S. Takano, A. Nakanishi, D. Uemura and Y. Hirata, Isolation and structure of a 334 nm UV-absorbing substance, porphyra-334 from the red algae, *Porphyra tenera* Kjellman, *Chem. Lett. (Chem. Soc. Jpn.)*, 1979, **26**, 419–420.
21 A. Defoin, R. Defoin-Straatmann, K. Hildenbrand, E. Bittersmann, D. Kreft and H. J. Kuhn, A new liquid actinometer: quantum yield and photo-CIDNP study of phenylglyoxylic acid in aqueous solution, *J. Photochem.*, 1986, **33**, 237–255.
22 D. E. Eaton, (IUPAC) Reference materials for fluorescence measurement, *Pure Appl. Chem.*, 1988, **60**, 1107–1114.
23 M. A. Brusa, M. S. Churio, M. A. Grela, S. G. Bertolotti and C. M. Previtali, Reaction volume and reaction enthalpy upon aqueous peroxodisulfate dissociation: $S_2O_8^{2-} \rightarrow 2\,SO_4^{\bullet -}$, *Phys. Chem. Chem. Phys.*, 2000, **2**, 2383–2387.
24 S. Abruzzetti, C. Viappiani, D. H. Murgida, R. Erra-Balsells and G. M. Bilmes, Non-toxic, water-soluble photocalorimetric reference compounds for UV and visible excitation, *Chem. Phys. Lett.*, 1999, **304**, 167–172.
25 K. Kasama, A. Takematsu and S. Aral, Photochemical reactions of triplet acetone with indole, purine, and pyrimidine derivates, *J. Phys. Chem.*, 1982, **86**, 2420–2427.
26 M. Terazima, Molecular volume and enthalpy changes associated with irreversible photoreaction, *J. Photochem. Photobiol. C: Photochem. Rev.*, 2002, **3**, 81–108.
27 D. C. Neckers, Rose bengal, *J. Photochem. Photobiol. A: Chem.*, 1989, **47**, 1–29.
28 H-J. Suh, H-W. Lee and J. Jung, Mycosporine glycine protects biological systems against photodynamic damage by quenching singlet oxygen with a high efficiency, *Photochem. Photobiol.*, 2003, **78**, 109–113.
29 F. Wilkinson, W. P. Helman and A. B. Ross, Rate constants for the decay and reactions of the lowest electronically excited singlet state of molecular oxygen in solution. An expanded and revised compilation, *J. Phys. Chem. Ref. Data*, 1995, **24**, 663–1021.
30 A. Gröniger and D-P. Häder, Stability of mycosporine-like amino acids, *Recent Res. Dev. Photochem. Photobiol.*, 2000, **4**, 247–252.
31 D. Karentz, Ultraviolet tolerance mechanisms in Antarctic marine organisms, in *Ultravolet radiation in Antarctica: Measurements and biological effects. Antarct. Res. Ser.*, ed. C. S. Weiler and P. A. Pénale, American Geophysical Union, Washington, DC, 1994, vol. 62, pp. 93–110.
32 N. J. Turro, *Modern Molecular Photochemistry*, Benjamin-Cummings Publishing Company Inc., Menlo Park, CA, 1978.
33 I. Laurion, F. Blouin and S. Roy, The quantitative filter technique for measuring phytoplankton absorption: Interference by MAAs in the UV waveband, *Limnol. Oceanogr.: Methods*, 2003, **1**, 1–9.
34 S. L. Murov, I. Carmichael and G. L. Hug, *Handbook of Photochemistry*, Marcel Dekker Inc., New York, 1993.
35 T. Gensch and S. Braslavsky, Volume changes related to triplet formation of water soluble Porphyrina. A laser-induced optoacoustic spectroscopy (LIOAS) study, *J. Phys. Chem. B*, 1997, **101**, 101–108.
36 S. E. Braslavsky, Volume changes on triplet production and quenching: time-resolved optoacoustic studies, *J. Photochem. Photobiol. A: Chem.*, 1996, **102**, 47–49.
37 T. Megyes, G. Schubert, M. Kovacs, T. Radnai, T. Grosz, I. Bako and A. Horvath, Structure and properties of the $[Ru(bpy)(CN)_4]^{2-}$ complex and its solvent environment: X-ray diffraction and density functional study, *J. Phys. Chem. A*, 2003, **107**, 9903–9909.
38 C. D. Borsarelli and S. E. Braslavsky, Volume changes correlate with enthalpy changes during the photoinduced formation of the ^{3}MLCT state of ruthenium(II) bipyridine cyano complexes in the presence of salts. A case of the entropy–enthalpy compensation effect, *J. Phys. Chem. B*, 1998, **102**, 6231–6238.
39 C. D. Borsarelli, S. G. Bertolotti and C. M. Previtali, Thermodynamic changes associated with the formation of the hydrated electron after photoionization of inorganic anion: time-resolved photoacoustic study, *Photochem. Photobiol. Sci.*, 2003, **2**, 791–795.